ORGANOMETALLICS

Article

pubs.acs.org/Organometallics

Open Access on 04/07/2015

Synthesis and Characterization of Dimethylbis(2-pyridyl)borate Nickel(II) Complexes: Unimolecular Square-Planar to Square-Planar Rotation around Nickel(II)

Jeff A. Celaje,[†] Megan K. Pennington-Boggio,[†] Robinson W. Flaig,[†] Michael G. Richmond,[‡] and Travis J. Williams*[,†]

[†]Loker Hydrocarbon Institute and Department of Chemistry, University of Southern California, Los Angeles, California, 90089-1661, United States

[‡]Department of Chemistry, University of North Texas, Denton, Texas, 76203-5017, United States

Supporting Information

ABSTRACT: The syntheses of novel dimethylbis(2-pyridyl)-borate nickel(II) complexes **4** and **6** are reported. These complexes were unambiguously characterized by X-ray analysis. In dichloromethane solvent, complex **4** undergoes a unique square-planar to square-planar rotation around the nickel(II) center, for which activation parameters of $\Delta H^{\ddagger}$ = 12.2(1) kcal mol^{-1} and $\Delta S^{\ddagger}$ = 0.8(5) eu were measured via NMR inversion recovery experiments. Complex **4** was also observed to isomerize via a relatively slow ring flip: $\Delta H^{\ddagger}$ = 15.0(2) kcal mol^{-1}; and $\Delta S^{\ddagger}$ = −4.2(7) eu. DFT studies support the experimentally measured rotation activation energy (cf. calculated $\Delta H^{\ddagger}$ = 11.1 kcal mol^{-1}) as well as the presence of a high-energy triplet intermediate (ΔH = 8.8 kcal mol^{-1}).

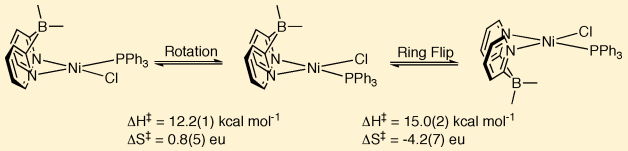

INTRODUCTION

A variety of low-valent nickel complexes have important reactivity in reactions ranging from the cycloisomerization of C=C[1] and C=O[2] π systems to the reduction of CO_2.[3] In line with the latter, we have recently observed that ammonia−borane dehydrogenation catalysts **1** and **2** (Figure 1A),[4] each bearing an anionic bidentate borate ligand, are capable of CO_2 reduction concurrent with ammonia−borane dehydrogenation. We therefore became interested in investigating the reactivity of other nickel complexes of the anionic bidentate ligand dimethylbis(2-pyridyl)borate (**3**; Figure 1B). In developing the synthesis of such complexes, we found an unexpected unimolecular square-planar to square-planar mutarotation of diamagnetic (borate)nickel(II) complex **4**. Rotations of this class, e.g. cis/trans isomerization of diamagnetic, square-planar late-metal complexes, are generally known not to proceed through unimolecular mechanisms.[5] Nickel(II) has a possible exception, however, in that these species can equilibrate between diamagnetic square-planar and paramagnetic tetrahedral configurations.[5a,6] Nonetheless, no case has been carefully documented wherein a diamagnetic square-planar metal undergoes facile, unimolecular ligand rotation.

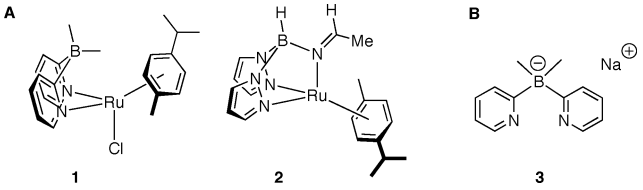

Figure 1. (A) Ru(II) complexes possessing an anionic bidentate borate ligand. (B) The dimethylbis(2-pyridyl)borate ligand **3**.

Herein we report the synthesis, characterization, and solution dynamics of the novel nickel(II) complexes (dimethylbis(2-pyridyl)borate)(triphenylphosphine)nickel(II) chloride (**4**) and (dimethylbis(2-pyridyl)borate)nickel(II) acetylacetonate (**6**) (Scheme 1). Complex **4** undergoes isomerization via two different mechanisms: (1) a unimolecular square-planar to square-planar rotation around the nickel(II) center and (2) a relatively slower ring flip. The activation parameters ($\Delta H^{\ddagger}$ and $\Delta S^{\ddagger}$) for both mechanisms were measured using ^{1}H NMR inversion recovery experiments.[7] Studies to show that rotation around the metal center is indeed unimolecular—not the usual associative or dissociative isomerization pathways that have been studied for many four-coordinate square planar metals[8]—are discussed.

RESULTS

Synthesis and Characterization of Complexes 4 and 6.

Complexes **4** and **6** were synthesized via simple metathesis reactions. The reaction of 1 equiv of bis(triphenylphosphine)-nickel(II) chloride with borate **3** in dichloromethane gives complex **4** in 71% isolated yield (Scheme 1). The formation of complex **4** is accompanied by formation of a small amount of the thermodynamically favored bis(borate) nickel complex **5**, which is known to form with facility when **3** is treated with

Received: February 17, 2014
Published: April 7, 2014

   dx.doi.org/10.1021/om500173j | Organometallics 2014, 33, 2019−2026

Scheme 1. Syntheses of 4 and 6

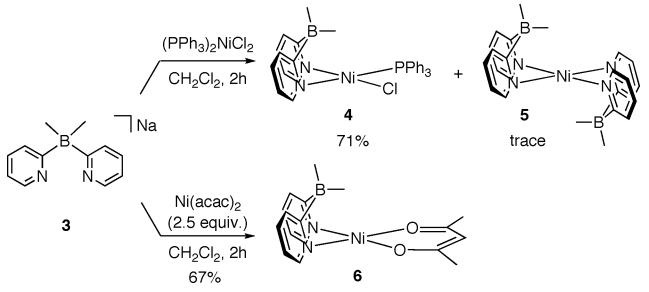

nickel(II) salts.[9] The acetylacetonate-ligated nickel complex **6** was readily prepared by treating an excess of $Ni(acac)_2$ (2.5 equiv) with sodium borate **3**, which yielded complex **6** (67%, Scheme 1). In contrast, the reactions of 1 equiv of either nickel(II) acetate tetrahydrate ($Ni(OAc)_2{\cdot}4H_2O$) or nickel(II) acetylacetonate ($Ni(acac)_2$) with **3** exclusively provide bis(borate) nickel complex **5**.

Both **4** and **6** were characterized by single-crystal X-ray crystallography (Figure 2). Both complexes are square planar.

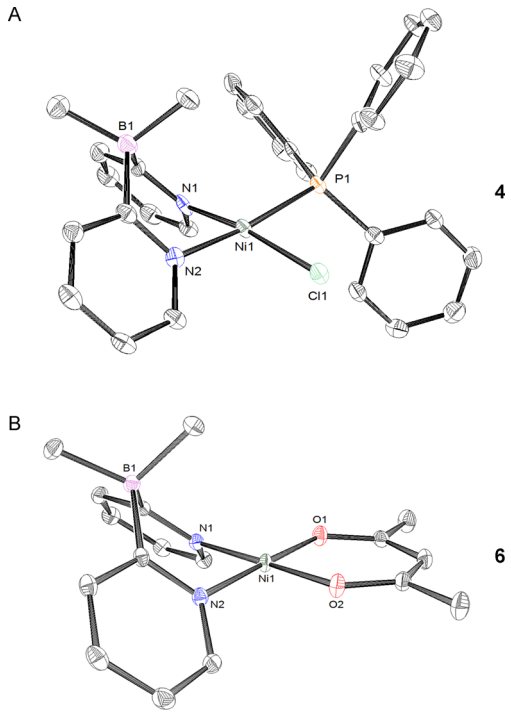

Figure 2. ORTEP diagrams of (A) complex **4** and (B) complex **6**. Ellipsoids are drawn at the 50% probability level. Complex **4** cocrystallizes with 0.5 equivalent of hexanes, which is omitted for clarity.

However, complex **4** exhibits a slight distortion. Whereas in complex **6** the sum of the bond angles around the nickel is 360.03(7)°, the sum of angles around nickel for complex **4** is 361.6(2)°, with the P−Ni−Cl plane tilted 14° relative to the N−Ni−N plane. An analogous nickel complex of the bidentate borate ligand dihydrobis(pyrazolyl)borate (Bp) has recently been reported and similarly adopts a square-planar structure.[10]

As in all previous complexes of **3**, the metal−chelate six-membered ring exhibits a boat conformation in both **4** and **6**.[4,11] The dihedral angle between metal and pyridine planes in complex **6** is 53.3(4)°. However, the dihedral angle in complex **4** is 47.9(2)°, indicating that the dimethylbis(2-pyridyl)borate ligand is tilted farther out of plane in complex **4**. Consistent with the observation of the increased tilt is the decreased distance between nickel and the carbon in the *endo*-configured (methyl)boron group in complex **4** (3.143 Å versus 3.171 Å in complex **6**). Complex **4** exhibits the expected *trans* effect with the Ni−N bond *trans* to PPh_3 longer than that *trans* to the Cl^- (1.945(2) and 1.893(3) Å, respectively). On the other hand, Ni−N bonds are equivalent (1.8943(8) and 1.8955(8) Å), and the Ni−O bonds are similar (1.8567(7) and 1.8615(7) Å) in complex **6**. The Ni−N bond lengths in both **4** and **6** are consistent with those observed for **5** (1.906(2) and 1.902(2) Å).[9]

Low-Temperature NMR Studies on Nickel Complex 4. The ^1H NMR spectrum of nickel complex **4** in CD_2Cl_2 at 25 °C shows that **4** is predominantly diamagnetic in solution. Further, it undergoes a dynamic process in solution, which is observed in variable-temperature (VT) NMR studies (Figure 3). Whereas the pyridyl α hydrogens of the bound dimethylbis(2-pyridyl)borate ligand give a coalesced singlet (δ 8.55 ppm) at 25 °C, two distinct singlets are observed at lower temperatures (i.e., δ 8.12 and 8.82 ppm at −40 °C). This means that complex **4** is isomerizing in solution (Figure 4A). A similar isomerization has been observed for an analogous Bp complex, **7** (Figure 4B).[10]

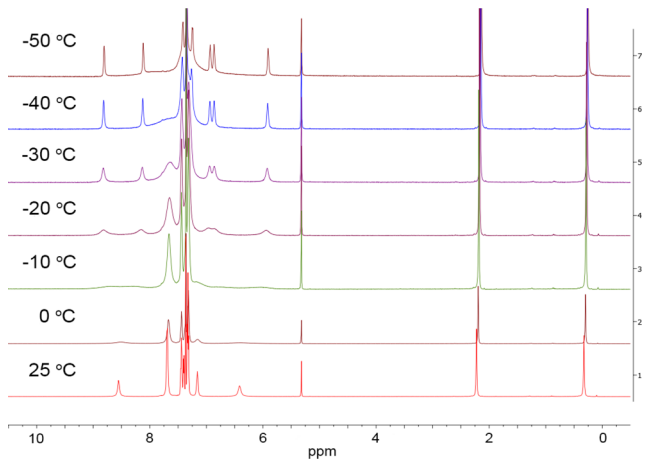

Figure 3. Variable-temperature ^1H NMR spectra of complex **4**.

Isomerization of square-planar complexes usually proceeds via either an associative or a dissociative mechanism (Scheme 2, vide infra).[8] However, we were intrigued by the possibility that we were observing isomerization via a mechanism involving a unimolecular (first-order) square-planar to square-planar

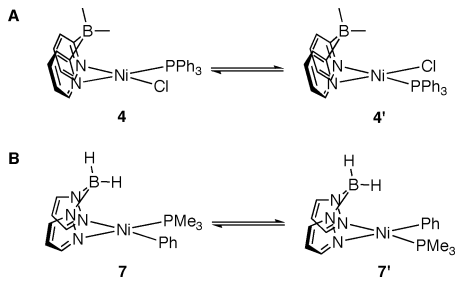

Figure 4. (A) Observed isomerization in complex **4**. (B) Isomerization of the dihydrobis(pyrazolyl)borate (Bp) complex **7**.[10]

dx.doi.org/10.1021/om500173j | *Organometallics* 2014, 33, 2019−2026

Scheme 2. Possible Mechanisms of Isomerization[a]

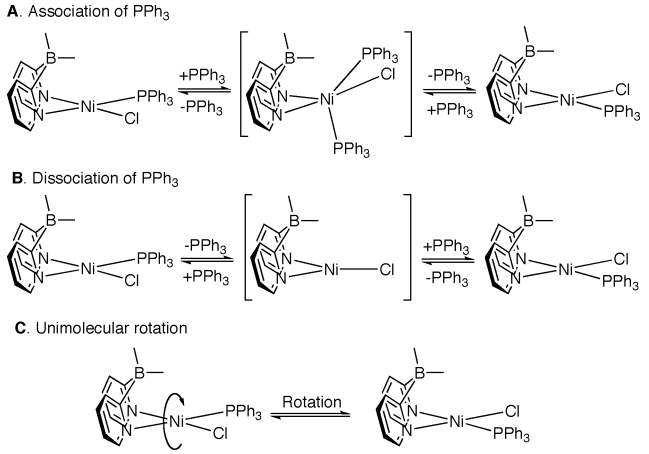

[a]Proposed associative and dissociative mechanisms involving PPh_3 are shown, but it is possible that the other two ligands, Cl^- and **3**, could also be responsible for effecting either of these mechanisms.

rotation around a metal center. Such a process could explain the observation from the ^1H NMR VT studies.

Kinetic Studies of the Conformational Dynamics of 4. To show that neither an associative nor dissociative mechanism is responsible for the isomerization of nickel **4**, we analyzed the dependence of the rate of isomerization with respect to the three ligands present in **4**: PPh_3, chloride, and **3**.

The ^1H NMR spectrum of nickel **4** at −40 °C shows well-differentiated pyridyl α hydrogens of the borate ligand (Figure 5). This presents an ideal opportunity to use ^1H NMR

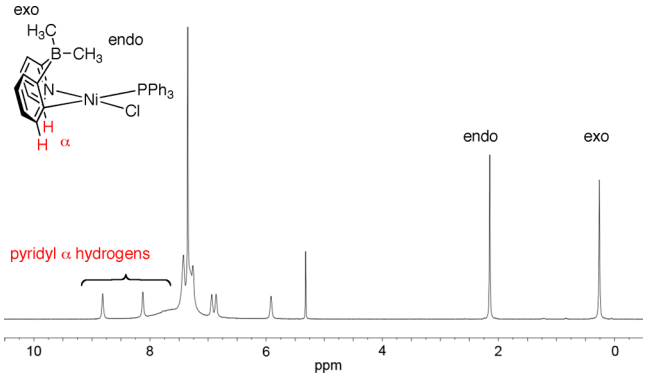

Figure 5. ^1H NMR spectrum of nickel **4** at −40 °C. (Methyl)boron groups are assigned by 1D-NOESY spectroscopy.

inversion recovery experiments to determine the rate of this isomerization. For example, when the pyridyl proton at 8.82 ppm is pulsed (selectively labeled by inversion), magnetization transfer to the pyridyl proton at 8.12 ppm can be observed. By acquisition of data with different mixing times, a rate constant for the isomerization can be obtained.[7]

Rate Dependence on PPh_3. The rate constants for the isomerization of **4** as a function of $[PPh_3]$ at −41.1 °C were obtained by using ^1H NMR inversion recovery experiments and fitting the data into CIFIT.[7] A plot of ln k_{obs} vs ln $[PPh_3]$ (Figure 6, left) shows that the rate of isomerization is independent of $[PPh_3]$. The rate of isomerization was unchanged upon addition of up to 10 equiv of PPh_3, and the slope of the ln/ln plot comparing the concentration of PPh_3

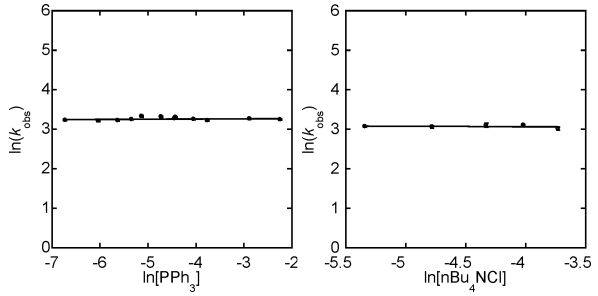

Figure 6. ln/ln plots of the dependence of isomerization rate of **4** on $[PPh_3]$ (left) and $[Cl^-]$ (right). For the plot on the left, inversion recovery data were collected at −41.1 °C using a 12 mM CD_2Cl_2 solution of **4** with $[PPh_3]$ ranging from 0.1 to 10.0 equiv. Slope = 0.00(1). For the plot on the right, inversion recovery data were collected at −43.0 °C using a 12 mM CD_2Cl_2 solution of **4** with $[(n\text{-}Bu)_4NCl]$ ranging among 0.4, 0.7, 1.1, 1.5, and 2.0 equiv versus Ni atom. Slope = −0.01(3).

with the observed rate of rotation had a slope of 0.0, which indicates that PPh_3 is of kinetic order 0.0 in the rotation mechanism.

Also, to ensure that PPh_3 exchange is not occurring, we performed a ^{31}P NMR inversion recovery study to see whether magnetization transfer from coordinated PPh_3 to free PPh_3 would occur. No magnetization transfer was observed at −42.4 °C (Figure 7), indicating that PPh_3 exchange is indeed not occurring at a temperature where rotation is fast: $t_{1/2}$ = 30 ms.

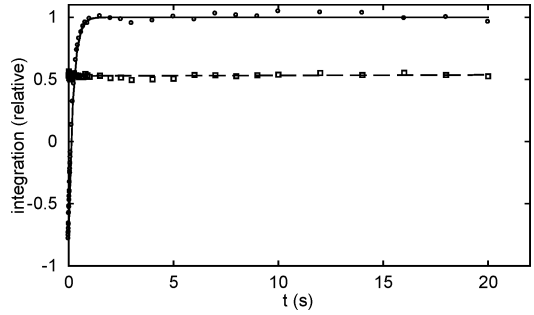

Figure 7. ^{31}P NMR inversion recovery experiment at −42.4 °C. Data were collected using a 12 mM CD_2Cl_2 solution of **4** with 0.5 equiv of added PPh_3: (○) coordinated PPh_3, $\delta(^{31}P)$ 12.60, ^{31}P T_1 = 213(3) ms; (□) free PPh_3;, $\delta(^{31}P)$ −7.23; linear slope 0.00(0).

Rate Dependence on Chloride. The rate of isomerization of **4** is also independent of the concentration of the chloride ligand (Figure 6, right). Because of the insolubility of the chloride anion in CD_2Cl_2, the isomerization is unlikely to be proceeding via a chloride dissociation mechanism. We nonetheless examined the rate of isomerization in the presence of tetra-*n*-butylammonium chloride ($(n\text{-}Bu)_4NCl$), a soluble source of chloride. Addition of $(n\text{-}Bu)_4NCl$ leads to a reaction wherein a small portion of an unidentified paramagnetic species is formed; regardless, **4** is observed in the ^1H NMR spectrum, and we recorded rate constants for the rotation in the presence of up to 2 equiv of $(n\text{-}Bu)_4NCl$. The rate of isomerization was unchanged by the presence of excess $(n\text{-}Bu)_4NCl$ (Figure 6, right). We also examined the rate of isomerization in the presence of excess LiCl, which is insoluble in CD_2Cl_2 and does not react with **4**. The rate of isomerization at −42.0 °C is unaffected by addition of an excess of LiCl (see the Supporting Information).

dx.doi.org/10.1021/om500173j | *Organometallics* 2014, 33, 2019−2026

While the dissociation of the chloride ligand to form a positively charged tricoordinate intermediate in a noncoordinating solvent (CD_2Cl_2) is unlikely, if the chloride ligand is dissociating from **4**, addition of thallium triflate should lead to formation of TlCl and to the removal of chloride from the coordination sphere of **4**. To test for this situation, we treated a solution of **4** with 2 mol equiv of Tl(OTf). The ^{1}H NMR spectrum of this sample is unaltered by the addition of Tl(OTf): **4** is stable in the presence of Tl(OTf) at room temperature for days, which indicates that the Cl^- ligand does not dissociate. Moreover, the presence of 2 equiv of Tl(OTf) does not alter the rate of isomerization at −42.0 °C (23.1(4) s^{-1} immediately after addition; 23.5(6) s^{-1} 4 days after addition).

Consideration of Borate 3 and Observation of a Second, Relatively Slower Isomerization Pathway. A mechanism of isomerization involving (a) dissociation of one of the pyridine rings of ligand **3**, followed by (b) rotation around the Ni−N bond of the bound pyridine, and then (c) recoordination of the free pyridine ring (Scheme 3) can be envisaged. This process leads to an isomerized product equivalent to an isomerized product of a ring flip. Since the two (methyl)boron groups are differentiated in the ^{1}H NMR spectrum of **4** (singlets at 2.22 and 0.32 ppm, Figure 5), inversion recovery experiments to measure the rate of this process are possible. When an ^{1}H NMR inversion recovery experiment is performed at −40 °C, no magnetization transfer is observed from one methyl group to the other. Even at 0 °C, the magnetization transfer is too slow to permit measurement of a rate constant. Only at 13.7 °C were we able to obtain a rate constant: k_{obs} = 2.69(4) s^{-1}. This ring flip is therefore a different, slower isomerization pathway for nickel **4** (Scheme 4). Since this separate process is much slower than the rotation, we find that the observed rotation behavior cannot be accounted for on the basis of a ring flip.

Scheme 3. Possible Mechanism of Isomerization Involving Dissociation of Ligand 3[a]

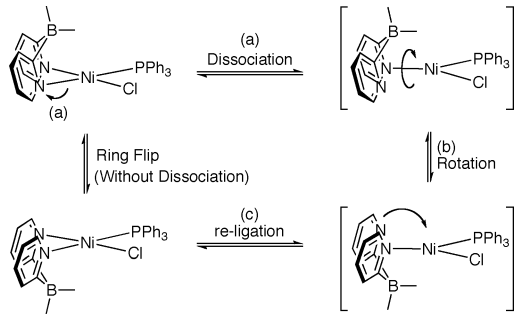

[a]Ring flip is possible with or without initial dissociation of a pyridyl nitrogen. The measured rate of ring flip is slower than the rate of rotation by greater than 2 orders of magnitude.

Activation Parameters for Square-Planar Rotation and Ring Flip. To determine activation parameters, we used Eyring plots constructed from rate constants obtained by NMR inversion recovery experiments. For the square-planar rotation of **4**, we obtained values of $\Delta H^{\ddagger}$ = 12.2(1) kcal mol^{-1} and $\Delta S^{\ddagger}$ = 0.8(5) eu (Figure 8, left). For the ring flip, we measured values of $\Delta H^{\ddagger}$ = 15.0(2) kcal mol^{-1} and $\Delta S^{\ddagger}$ = −4.2(7) eu (Figure 8, right).[12,13] Note that the rates for rotation and ring flip differ by greater than 2 orders of magnitude (ca. 3 kcal/mol), with rotation being faster.

Scheme 4. Ring Flip Places the (Methyl)boron Groups of 4 in a Different Chemical Environment, Whereas Rotation Places Them in the Same Chemical Environment[a]

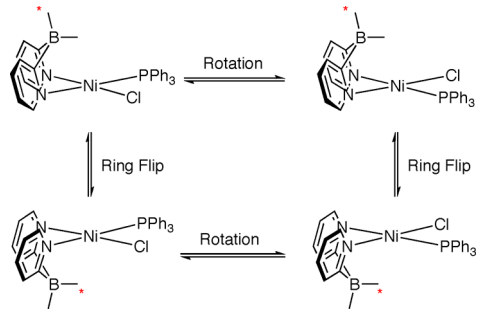

[a]Magnetization transfer between *endo* and *exo* (methyl)boron groups is not observed at low temperatures because rotation places the methyl groups in the same chemical environment (by symmetry). In contrast, magnetization transfer can be observed at higher temperatures via ring flip.

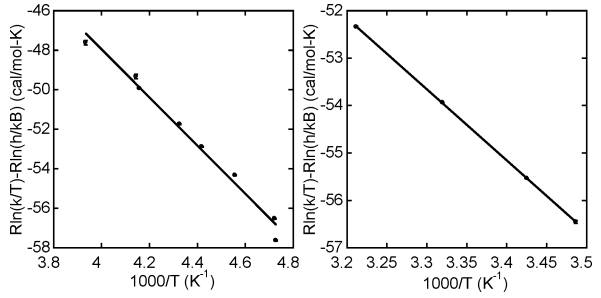

Figure 8. Eyring plots for unimolecular rotation (left) and ring flip (right). For the plot on the left, inversion recovery data were collected using a 12 mM CD_2Cl_2 solution of **4** at −61.6, −61.4, −53.7, −46.8, −42.0, −32.6, −31.8, and −18.9 °C. $\Delta H^{\ddagger}$ = 12.2(1) kcal mol^{-1} and $\Delta S^{\ddagger}$ = 0.8(5) eu.[13] For the plot on the right, data were collected using a 12 mM CD_2Cl_2 solution of **4** at 13.7, 18.8, 28.1, and 38.2 °C. $\Delta H^{\ddagger}$ = 15.0(2) kcal mol^{-1} and $\Delta S^{\ddagger}$ = −4.2(7) eu.[13]

DFT Studies. The potential energy surface for rotational isomerization of the PMe_3 analogue of nickel **4** was evaluated computationally by DFT (Figure 9). The geometry-optimized structure of singlet **A** shows an excellent correspondence with the experimentally determined structure of **4**, which reinforces the use of this model as a probe for the isomerization in **4**.

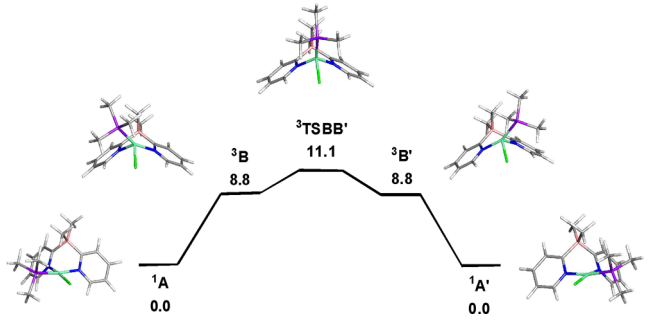

Figure 9. PBE-optimized structures for the singlet (^{1}**A**) and triplet (^{3}**B**) species $[Me_2B(2\text{-}py)_2]NiCl(PMe_3)$ and the potential energy surface for the low-energy rotational isomerization of the PMe_3 and Cl ligands via ^{3}**TSBB′**. Energy values (ΔH) are given in kcal mol^{-1}.

dx.doi.org/10.1021/om500173j | *Organometallics* 2014, 33, 2019−2026

Diamagnetic **A** is the thermodynamically preferred isomer, and the pseudotetrahedral triplet **B** lies 8.8 kcal mol^{-1} above **A**. The computed free energy difference between **A** and **B** is 9.9 kcal mol^{-1}, leading to a K_{eq} value of ca. 10^{-8} for the triplet at room temperature, whose concentration is negligible and is in keeping with the silent EPR spectrum and magnetic susceptibility data recorded for **4** (vide infra). **B** is formed by a directionally specific clockwise rotation of the PMe_3 and Cl ligands in **A**, and continued rotation of these groups furnishes the transition structure **TSBB'** that exhibits C_s symmetry. Here the PMe_3 ligand maintains a proximal orientation with respect to the BMe_2 moiety throughout the isomerization; PMe_3 rotation away from the BMe_2 moiety and under the pyridyl rings leads to deleterious steric interactions. The computed enthalpic barrier of 11.1 kcal mol^{-1} closely matches the experimentally determined $\Delta H^{\ddagger}$ value for the process.

DISCUSSION

Possible Mechanisms of Isomerization. While no example of a unimolecular square-planar to square-planar rotation around a diamagnetic late-metal complex has been documented, prior studies show that such a rotation is possible for some nickel(II) systems. In noncoordinating solvents, four-coordinate d^8 nickel(II) complexes that exist in equilibrium as diamagnetic ($S = 0$) square planar and paramagnetic ($S = 1$) tetrahedral isomers have been well documented.[14] Eaton used the Woodward−Hoffmann rules to obtain the selection rules for isomerization of four-coordinate nickel(II) complexes and showed that the isomerization from square planar to tetrahedral should be a facile, thermally allowed process.[15] Likewise, using orbital correspondence analysis with maximum symmetry, Halevi and Knorr showed that tetrahedral triplet to planar singlet isomerizations of nickel(II) complexes accompanied by a spin flip are thermally allowed.[16] Indeed, the reported rates of isomerizations for several nickel(II) species are fast. For example, lifetimes of 10^{-5} s for each isomer have been measured for nickel(II) aminotroponeiminates,[14a] bis(salicylaldimine)nickel(II),[14b,c] and a series of bis(*n*-alkyldiphenylphosphine)nickel(II) dihalides.[14k] Moreover, the racemization of optically active diastereomeric (Δ and Λ) nickel(II) species was noted to be so fast that each diastereomer could not be observed by NMR.[14g,k] Thermodynamic studies show that this equilibrium is affected by ligand sterics, with the presence of bulkier ligands favoring formation of the usually less thermodynamically stable tetrahedral complex.[14] The effects on equilibrium by electronic factors are also important.[14a,j−l,p]

Although the literature suggests that rotation around a square-planar nickel(II) center is possible, only two classes of isomerization have been mechanistically characterized by studies of a large number of diamagnetic square-planar complexes, (1) associative and (2) dissociative, with associative mechanisms being more frequently reported.[8,17] Associative isomerization can proceed through two mechanisms: Berry pseudorotation and consecutive displacement. These associative isomerizations initiate by coordination of a catalytic ligand to metal to form a five-coordinate intermediate. This ligand can be an added base, solvent, or any metal-coordinating group. In the case of the Berry pseudorotation, the five-coordinate intermediate isomerizes to a trigonal bipyramid in which ligands can be isomerized, followed by dissociation of the catalytic ligand. In the consecutive displacement mechanism, coordination of the catalytic ligand is followed by either loss of an anionic ligand to generate a cationic metal species or dissociation of a neutral ligand to generate a neutral metal species. This is followed by recoordination of the original ligand and loss of the catalytic ligand. Some authors contend that displacement of a neutral ligand would not result in isomerization, due to the stereospecific nature of ligand substitutions,[8] while others claim to have definitively proven the existence of the neutral intermediate.[18] There is also debate about the existence of complexes which isomerize via a pseudorotation mechanism and disagreement about what evidence definitively proves a pseudorotation mechanism over a consecutive displacement mechanism.

While it is difficult to distinguish among the mechanisms of associative isomerization, it is straightforward to classify an isomerization as associative: by showing first-order rate dependence on added ligand. In contrast, dissociative isomerization proceeds through loss of a ligand to generate a three-coordinate complex. Diminution of rate in the presence of excess ligand, isomerization in the absence of potential ligands, including coordinating solvents, and positive $\Delta S^{\ddagger}$ are often taken as evidence of a dissociative process, but evidence of the existence of a three-coordinate intermediate is required confidently to conclude a dissociative mechanism.

Unimolecular Rotation of Nickel 4. Previous studies on square-planar to tetrahedral equilibria of nickel(II) complexes, which include molecular orbital analyses, indicate the possibility of isomerization via a unimolecular square-planar to square-planar rotation around a nickel center (i.e., a 90° rotation from square planar to tetrahedral followed by another 90° rotation from tetrahedral to square planar).[14−16] However, no study that systematically shows—by excluding the associative or dissociative isomerization pathways—unimolecular rotation around a diamagnetic square-planar nickel complex has been reported. These cases involve equilibrium between two observable geometric isomers at nickel: a diamagnetic square-planar complex and a paramagnetic tetrahedral complex. Moreover, ligands in some of these complexes are known to be substitutionally labile. For example, in the presence of excess phosphine, bis(*n*-alkyldiphenylphosphine)nickel(II) dihalides undergo phosphine exchange to give a second-order ligand exchange mechanism that contributes to the rate of isomerization.[14k] Similarly, bis(salicylaldimine)nickel(II)[14d] and bis(β-ketoimine)nickel(II)[14g] complexes undergo facile mixed ligand exchange.

The studies mentioned in the Results show that the rotation of complex **4** in a noncoordinating solvent involves neither an associative nor a dissociative mechanism at the temperatures studied. The most likely ligand to be involved in associative or dissociative isomerization is PPh_3. The observation that the rate of isomerization is independent of [PPh_3] excludes an associative process and provides evidence against a dissociative process. Moreover, ^{31}P NMR inversion recovery experiments show that, in the presence of excess PPh_3, exchange between coordinated and free PPh_3 is not occurring, thus excluding a dissociative mechanism involving PPh_3.

The rate of isomerization is also unaffected by the presence of excess $(n\text{-Bu})_4NCl$ or LiCl, which precludes an associative mechanism with respect to the chloride ligand. This result is not surprising, given the low dielectric constant of CD_2Cl_2, which disfavors charge separation. A dissociative process is ruled out by the fact that addition of 2 equiv of Tl(OTf) does not alter the ^{1}H NMR spectrum of complex **4**. If dissociation of the chloride ligand is occurring, the addition of thallium, which

dx.doi.org/10.1021/om500173j | *Organometallics* 2014, 33, 2019−2026

has strong affinity for halides, would sequester free chloride in solution and alter the ^{1}H NMR spectrum. Moreover, the rate of isomerization at −42.0 °C was unaffected by the presence of 2 equiv of Tl(OTf), even after the solution was allowed to stand at room temperature for 4 days. This shows that (a) the structure and (b) the conformational dynamics of **4** are unaffected by the presence of Tl(OTf), which is inconsistent with chloride dissociation under these conditions.

Studies of the dependence of the rate of isomerization on [**3**] are not possible because addition of excess **3** results in fast formation of bis(borate) nickel complex **5**. However, the isomerization proceeds in the absence of excess **3**; thus, an associative process involving **3** is unlikely. Also, the $\Delta S^{\ddagger}$ value for isomerization (0.8(5) eu) is inconsistent with ligand association (which generally has $\Delta S^{\ddagger}$ = −10 to −15 eu).[19]

Likewise, the $\Delta S^{\ddagger}$ value is too small to be consistent with ligand dissociation (which generally has $\Delta S^{\ddagger}$ = 10 to 15 eu).[19] For example, the $\Delta S^{\ddagger}$ values for the dissociative substitution of CO in $Ni(CO)_4$ range from +8 to +13 eu, depending on solvent.[20] Moreover, the bond enthalpy of a Ni−N(pyridine) bond (ca. 26 kcal mol^{-1})[21] is much higher than the measured $\Delta H^{\ddagger}$ value for the isomerization (12.2(1) kcal mol^{-1}), which indicates that the Ni−N bond is not broken during the isomerization process. Furthermore, an isomerization involving the dissociation of **3** (Scheme 3), which leads to a product equivalent to a ring flip product, was considered. This process was found to be a separate, slower isomerization pathway: ring flip is >100-fold slower than rotation at a given temperature. The $\Delta S^{\ddagger}$ for the ring flip (−4.2(7) eu) indicates a more ordered transition state and thus argues against a dissociative mechanism (i.e., the ring flip occurs without hemidissociation of **3**). If hemidissociation is not occurring at higher temperatures where the ring flip is observed (as high as 38.2 °C), then it is unlikely that hemidissociation is occurring at temperatures as low as −61.6 °C, where rotation is observed. Finally, the presence of excess PPh_3 should affect the rate of isomerization if hemidissociation is occurring, but this is not observed. On the basis of these observations, we believe that association or dissociation of ligand **3** is not involved in the rotation mechanism.

A further associative rotation mechanism that fits these kinetic data is one that involves formation of an agostic Ni−HC interaction[22] to the *endo* (methyl)boron group to generate a transient five-coordinate nickel center. We believe that such an agostic interaction is not forming for three key reasons. (1) The ^{1}H NMR peak width of the *endo*-positioned (methyl)boron group in **4** is invariant over a range of 75 °C (6.9 ± 1.0 Hz, Figure 3). (2) The ^{1}H chemical shift of the same is invariant over the same temperature range: 2.22 ± 0.09 ppm. (3) The solid-state Ni−H distance is 2.43 Å, which is longer than those observed for agostic interactions between this ligand and ruthenium(II) (1.72 Å)[4a] or platinum(IV) (2.02 Å).[11b] Moreover, the agostic Ni−H distance in a (NacNac)Ni(κ^2-C_2H_5) complex is 1.66 Å,[23] which is far smaller than our observed Ni−H distance (NacNac = *N*,*N*′-(2,6-$(CH_3)_2C_6H_3)_2CH_3C(N)CHC(N)CH_3$ anion). Whereas none of our observations are consistent with known agostic complexes involving borate **3**, we predict that no agostic intermediate is involved in the unimolecular rotation of **4**.

As corroborated by DFT calculations, the unimolecular rotation of **4** involves the intermediacy of a paramagnetic, tetrahedral (or pseudotetrahedral) complex, but this species is not present in an observable concentration. For example, the phosphine crossover experiment shown in Figure 7 shows that, under the isomerization conditions, the ^{31}P NMR integrations of **4** and PPh_3 in solution match the portions added to the sample. This provides evidence that there is not a large portion of phosphine associated with an NMR-invisible paramagnetic species. Furthermore, an EPR spectrum of **4** (X-band, 25 °C, toluene) showed no signals.[24] Moreover, whereas the paramagnetic susceptibility of many nickel(II) complexes which exhibit square-planar to tetrahedral equilibria can be measured using the Evans method,[14a,j−l] we observe no paramagnetic susceptibility of complex **4** even at high concentrations (127 mM, 25 °C; see the Supporting Information) using this method.[25]

DFT studies confirm the presence of a high-energy triplet intermediate on the potential energy surface for the rotational exchange of the phosphine and chlorine ligands in **4**. These computational studies show that the enthalpic barrier for rotation in the PMe_3 analogue ($\Delta H^{\ddagger}$ = 11.1 kcal mol^{-1}) of nickel **4** is very close to that value experimentally measured for nickel **4**. The presence of a high-energy triplet intermediate (ΔH = 8.8 kcal mol^{-1}) was also corroborated by these studies.

On the basis of the forgoing evidence, we believe that the internal rotation of **4** is the first documented case of a unimolecular square-planar to square-planar rotation around a late-metal center. We believe that this mechanism proceeds through a high-energy paramagnetic tetrahedral (or pseudotetrahedral) nickel(II) intermediate species. We propose, however, that no ligand coordination or dissociation, including agostic coordination of a (methyl)boron group, is requisite to the mechanism.

■ CONCLUSION

The novel dimethylbis(2-pyridyl)borate nickel complexes **4** and **6** were synthesized and characterized. The solution dynamics of complex **4** were studied, and it was found to isomerize via two different mechanisms: (a) a unimolecular square-planar to square-planar rotation around the nickel center and (b) a relatively slower ring flip. The activation parameters for each isomerization pathway were measured using ^{1}H NMR inversion recovery experiments. The barrier for rotation ($\Delta H^{\ddagger}$ = 12.2(1) kcal mol^{-1} and $\Delta S^{\ddagger}$ = 0.8(5) eu) is lower than the barrier for the ring flip ($\Delta H^{\ddagger}$ = 15.0(2) kcal mol^{-1} and $\Delta S^{\ddagger}$ = −4.2(7) eu), as expected. This study is the first to systematically show (by excluding the associative and dissociative pathways) that a 180° rotation around a square-planar nickel center is a viable mechanism of isomerization.

■ EXPERIMENTAL SECTION

General Procedures. All air- and water-sensitive procedures were carried out either in a Vacuum Atmospheres glovebox under nitrogen (2−10 ppm O_2 for all manipulations) or using standard Schlenk techniques under nitrogen. Deuterated NMR solvents were purchased from Cambridge Isotopes Laboratories. Dichloromethane, ethyl ether, and hexanes were purchased from VWR and dried in a J. C. Meyer solvent purification system with alumina/copper(II) oxide columns, benzene (EMD) was dried by distillation over sodium−benzophenone ketyl, and bis(triphenylphosphine)nickel(II) chloride and nickel(II) acetylacetonate were purchased from Strem and used as received.

NMR spectra were recorded on a Varian VNMRS 500 or VNMRS 600 spectrometer. All chemical shifts are reported in units of ppm and referenced to the residual ^{1}H or ^{13}C solvent peak and line-listed according to (s) singlet, (bs) broad singlet, (d) doublet, (t) triplet, (dd) doublet of doublets, etc. ^{13}C spectra are delimited by carbon peaks, not carbon count. ^{11}B and ^{31}P chemical shifts are referenced to

dx.doi.org/10.1021/om500173j | *Organometallics* 2014, 33, 2019−2026

the lock channel. Air-sensitive NMR spectra were taken in 8 in. J. Young tubes (Wilmad or Norell) with Teflon valve plugs. Inversion recovery kinetics data were fitted using CIFIT 2.0 by Alex Bain.[7b] Temperatures for NMR experiments were calibrated using an external methanol standard. Errors in Eyring parameters are calculated using the equations derived by Girolami et al.[13]

MALDI mass spectra were obtained on an Applied Biosystems Voyager spectrometer using the evaporated drop method on a coated 96-well plate. The matrix was anthracene. In a standard preparation, ca. 1 mg of analyte and ca. 10 mg of matrix were dissolved in dry benzene and spotted on the plate with a glass capillary. Infrared spectra were recorded on a Bruker OPUS FTIR spectrometer. High-resolution ESI mass spectra were recorded at the University of California, Riverside. CHN elemental analyses were collected at the University of Illinois at Urbana−Champaign at the School of Chemical Sciences Microanalysis Laboratory.

Nickel Complex 4. In the drybox under nitrogen, $(PPh_3)_2NiCl_2$ (65.4 mg, 0.10 mmol) was dissolved in 10 mL of dry dichloromethane in a dry vial containing a Teflon stir bar. In another vial, $[(py)_2BMe_2]Na$[9] (22.0 mg, 0.10 mmol) was dissolved in 5 mL of dry dichloromethane and added slowly to the $(PPh_3)_2NiCl_2$ solution. The $[(py)_2BMe_2]Na$ vial was rinsed with 5 mL of dichloromethane and added to the $(PPh_3)_2NiCl_2$ solution. The dark green solution turned brown and then orange upon addition of $[(py)_2BMe_2]Na$. The solution was stirred for 2 h and then filtered. The solvent was removed under reduced pressure. Dry diethyl ether was added to the residue, and the vial was sonicated briefly. The residue was then cooled using a cold well, and cold, dry hexanes was added. The suspension was filtered and washed with cold, dry ether. The suspension was dissolved with cold, dry benzene. The benzene was then removed by lyophilization to yield 39.5 mg (0.071 mmol, 71%) of $[(py)_2BMe_2]$-$Ni(PPh_3)Cl$ as a pale pink solid. Crystallization from dichloromethane and hexanes produced crystals suitable for X-ray crystallographic analysis.

^{1}H NMR (CD_2Cl_2, 600 MHz, 25 °C): δ 8.55 (br s, 2H), 7.77−7.61 (m, 6H), 7.44 (t, J = 7.3 Hz, 3H), 7.40 (d, J = 7.6 Hz, 2H), 7.33 (t, J = 7.6 Hz, 6H), 7.16 (br s, 2H), 6.41 (br s, 2H), 2.22 (s, 3H), 0.32 (s, 3H). ^{1}H NMR (CD_2Cl_2, 600 MHz, −40 °C): δ 8.82 (s, 1H), 8.12 (s, 1H), 8.02−7.02 (m, 18H), 6.94 (s, 1H), 6.86 (s, 1H), 5.92 (s, 1H), 2.15 (s, 3H), 0.26 (s, 3H). ^{13}C NMR (CD_2Cl_2, 150 MHz, 25 °C): δ 189.72 (br), 151.89, 135.07, 134.86, 131.08, 129.91, 128.91, 127.00, 119.75, 19.51 (br), 9.48 (br). ^{11}B NMR (CD_2Cl_2, 192 MHz): δ −12.68. ^{31}P NMR (CD_2Cl_2, 243 MHz, −40 °C): δ 12.42. MALDI: m/z 552.8941, calcd for $C_{30}H_{29}BClNiN_2P^+$ $[M]^+$ 552.1203. FT-IR (thin film/cm^{-1}): ν 3067.76, 2912.82, 2823.99, 1963.28, 1896.13, 1817.39, 1592.78, 1553.13, 149.62, 1435.29, 1290.62, 1217.84, 1093.77, 1012.64, 744.01. Anal. Calcd for $C_{30}H_{29}BClNiN_2P$: C, 65.1; H, 5.28; N, 5.06. Found: C, 65.04; H, 5.47; N, 5.28.

Nickel Complex 6. In the drybox under nitrogen, $Ni(acac)_2$ (64.2 mg, 0.25 mmol) was suspended in 10 mL of dry dichloromethane in a dry vial containing a Teflon stir bar. In another dry vial, $[(py)_2BMe_2]Na$[9] (22.0 mg, 0.10 mmol) was dissolved in 5 mL of dichloromethane and added slowly to the solution of $Ni(acac)_2$. Another 5 mL of dichloromethane was used to rinse the vial and added slowly to the solution of $Ni(acac)_2$. The green solution turned orange on addition of $[(py)_2BMe_2]Na$. The solution was stirred for 2 h at room temperature and then filtered through Celite. The solvent was removed in vacuo. Dry hexanes (10 mL) was added to the residue, and the vial was treated with sonication briefly. The suspension was then cooled using a cold well, filtered, and washed with cold, dry hexanes. The solid was dried under vacuum to yield 23.7 mg (0.067 mmol, 67%) of $[(py)_2BMe_2]Ni(acac)$ as an orange solid. Crystallization from dichloromethane and hexanes produced crystals suitable for X-ray crystallographic analysis.

^{1}H NMR (CD_2Cl_2, 600 MHz): δ 8.30 (d, J = 5.6 Hz, 2H), 7.40 (d, J = 7.5 Hz, 2H), 7.34 (t, J = 7.3 Hz, 2H), 6.83 (t, J = 6.3 Hz, 2H), 5.55 (s, 1H), 2.27 (br s, 2H), 1.88 (s, 6H), 0.27 (br s, 3H). ^{13}C NMR (CD_2Cl_2, 150 MHz): δ 189.81 (q, J = 48 Hz) 188.11, 149.89, 135.23, 125.93, 119.71, 102.04, 26.09, 18.93 (br), 8.93 (br). ^{11}B NMR (CD_2Cl_2, 192 MHz): δ −12.68. MALDI: m/z 354.2477, calcd for $C_{17}H_{22}BN_2O_2Ni^+$ $[M]^+$ 354.1050. FT-IR (thin film/cm^{-1}): ν 2891.92, 2821.81, 1586.41, 1532.39, 1388.63, 1289.47, 122.57, 1159.73, 1015.71, 934.76, 788.67, 753.86, 738.46. HR-MS (+ESI): m/z 355.1129, calcd for $C_{17}H_{22}BN_2O_2Ni^+$ $[MH]^+$ 355.1122.

Computational Methodology and Modeling Details. The geometry optimizations reported here were performed with the DFT gradient-corrected correlation functional PBE, as implemented by the Gaussian 09 program package.[26] The Ni atom was described by a Stuttgart−Dresden effective core potential (ecp) and an SDD basis set, while the 6-31G(d′) basis set was employed for the remaining Cl, P, N, C, B, and H atoms.

All structures were fully optimized and evaluated for the correct number of imaginary frequencies through calculation of the vibrational frequencies, using the analytical Hessian (positive eigenvalues ground-state minima and one negative eigenvalue for a transition state). The computed frequencies were used to make zero-point and thermal corrections to the electronic energies, and the reported enthalpies are quoted in kcal/mol relative to singlet species **A**. The computed triplet species **B** and **TSBB′** revealed no significant spin contamination from higher order spin states. The geometry-optimized structures have been drawn with the JIMP2 molecular visualization and manipulation program.[27]

■ ASSOCIATED CONTENT

Ⓢ Supporting Information

Figures, tables, text, CIF, and .mol files giving graphical NMR data, NMR inversion recovery data, CIFIT plots for determination of rate constants, Eyring plots for determination of activation parameters, magnetic susceptibility data, crystallographic data for complexes **4** and **6**, complete ref 26, and atomic coordinates of the optimized stationary points **A** and **B** and the transition state **TSBB′**. This material is available free of charge via the Internet at http://pubs.acs.org. CCDC 984289 (**4**) and 984290 (**6**) contain supplementary crystallographic data for these compounds.

■ AUTHOR INFORMATION

Corresponding Author

*E-mail for T.J.W.: travisw@usc.edu.

Notes

The authors declare no competing financial interest.

■ ACKNOWLEDGMENTS

This work was sponsored by the NSF (CHE-1054910), the University of Southern California, the Loker Hydrocarbon Research Institute, the Hydrocarbon Research Foundation, the Robert A. Welch Foundation (Grant B-1093-MGR), and the Anton Burg Foundation. We thank the NSF (DBI-0821671, CHE-0741936, CHE-0840366, CHE-1048807) and the NIH (S10 RR25432) for analytical instrumentation and computational facilities. R.W.F. acknowledges NSF-REU support (CHE-1156836). We are grateful to A. Kershaw (NMR), Dr. R. Haiges (X-ray crystallography), X. Wu (EPR), and Dr. S. Zhang (EPR) for technical assistance. M.G.R. thanks Prof. Michael B. Hall (TAMU) for providing us a copy of his JIMP2 program, which was used to prepare the geometry-optimized structures reported here, and Dr. David A. Hrovat for helpful DFT discussions.

■ REFERENCES

(1) (a) Jolly, P. W. Nickel-Catalyzed Oligomerization of Alkenes and Related Reactions. In *Comprehensive Organometallic Chemistry*; Wilkinson, G., Stone, F. G. A., Abel, E. W., Eds.; Pergamon: New York, 1982; Vol. *8*, pp 615−712. (b) Jolly, P. W.; Wilke, G. *The Organic Chemistry of Nickel*; Academic: New York, 1974, 1975; Vols. *1*

and 2. (c) Heimbach, P.; Jolly, P. W. Wilke, G. In *Advances in Organometallic Chemistry*; Stone, F. G. A., West, R., Eds.; Academic: New York, 1970; Vol. 8, p 29. (d) Reed, H. W. B. *J. Chem. Soc.* **1954**, 1931−1941. (e) Yamamoto, Y. *Chem. Rev.* **2012**, *112*, 4736−4769.

(2) (a) *Modern Organonickel Chemistry*; Tamaru, Y., Ed.; Wiley-VCH: Weinheim, Germany, 2005. (b) Oblinger, E.; Montgomery, J. *J. Am. Chem. Soc.* **1997**, *119*, 9065−9066. (c) Kimura, M.; Ezoe, A.; Shibata, K; Tamaru, Y. *J. Am. Chem. Soc.* **1998**, *120*, 4033−4034. (d) Takimoto, M.; Hiraga, Y.; Sato, Y.; Mori, M. *Tetrahedron Lett.* **1998**, 4543−4546. (e) Kimura, M.; Fujimatsu, H.; Ezoe, A.; Shibata, K; Shimizu, M.; Matsumoto, S.; Tamaru, Y. *Angew. Chem., Int. Ed.* **1999**, *38*, 397−400. (f) Kang, S.; Yoon, S. *Chem. Commun.* **2002**, 2634−2635. (g) Miller, K.; Huang, W.; Jamison, T. F. *J. Am. Chem. Soc.* **2003**, *125*, 3442−3443. (h) Montgomery, J. *Angew. Chem., Int. Ed.* **2004**, *43*, 3890−3908. (i) Ogoshi, S.; Oka, M.; Kurosawa, H. *J. Am. Chem. Soc.* **2004**, *126*, 11802−11803. (j) Ogoshi, S.; Ueta, M.; Arai, T.; Kurosawa, H. *J. Am. Chem. Soc.* **2005**, *127*, 12810−12811.

(3) (a) Chakraborty, S.; Zhang, J.; Krause, J. A.; Guan, H. *J. Am. Chem. Soc.* **2010**, *132*, 8872−8873. (b) Chakraborty, S.; Patel, Y. J.; Krause, J. A.; Guan, H. *Polyhedron* **2012**, *32*, 30−34. (c) Chakraborty, S.; Zhang, J.; Patel, Y. J.; Krause, J. A.; Guan, H. *Inorg. Chem.* **2013**, *52*, 37−47. (d) Schmeier, T. J.; Hazari, N.; Incarvito, C. D.; Raskatov, J. A. *Chem. Commun.* **2011**, *47*, 1824−1826. (e) Wu, J.; Hazari, N.; Incarvito, C. D. *Organometallics* **2013**, *32*, 300−308. (f) Vogt, M.; Rivada-Wheelaghan, O.; Iron, M. A.; Leitus, G.; Diskin-Posner, Y.; Shimon, L. J. W.; Ben-David, Y.; Milstein, D. *Organometallics* **2013**, *32*, 300−308.

(4) (a) Conley, B.; Williams, T. J. *J. Am. Chem. Soc.* **2010**, *132*, 1764−1765. (b) Conley, B. L.; Guess, D.; Williams, T. J. *J. Am. Chem. Soc.* **2011**, *133*, 14212−14215. (c) Lu, Z.; Williams, T. J. *Chem. Commun.* **2014**, DOI: 10.1039/C3CC47384H.

(5) (a) Basolo, F.; Pearson, R. G. *Mechanisms of Inorganic Reactions*, 2nd ed.; Wiley: New York, 1958; pp 423−435. (b) Redfield, D. A.; Nelson, J. H. *J. Am. Chem. Soc.* **1974**, *96*, 6219−6220.

(6) Cotton, F. A.; Wilkinson, G. *Advanced Inorganic Chemistry: A Comprehensive Text*, 4th ed.; Wiley: New York, 1980; pp 791−794.

(7) (a) Williams, T. J.; Kershaw, A. D.; Li, V.; Wu, X. *J. Chem. Educ.* **2011**, *88*, 665−669. (b) Bain, A. D.; Cramer, J. A. *J. Magn. Reson.* **1996**, *118 A*, 21−27.

(8) For a review, see: Anderson, G. K.; Cross, R. J. *Chem. Soc. Rev.* **1980**, *9*, 185−215.

(9) Hodgkins, T. G.; Powell, D. R. *Inorg. Chem.* **1996**, *35*, 2140−2148.

(10) Gutierrez, E.; Hudson, S. A.; Monge, A.; Nicasio, M. C.; Paneque, M.; Ruiz, C. *J. Organomet. Chem.* **1998**, *551*, 215−227.

(11) (a) Khaskin, E.; Zavalij, P. Y.; Vedernikov, A. N. *J. Am. Chem. Soc.* **2006**, *128*, 13054−13055. (b) Khaskin, E.; Zavalij, P. Y.; Vedernikov, A. N. *Angew. Chem., Int. Ed.* **2007**, *46*, 6309−6312. (c) Khaskin, E.; Zavalij, P. Y.; Vedernikov, A. N. *J. Am. Chem. Soc.* **2008**, *130*, 10088−10089. (d) Khaskin, E.; Lew, D. L.; Pal, S.; Vedernikov, A. N. *Chem. Commun.* **2009**, 6270−6272.

(12) Because CD_2Cl_2 boils at 39 °C, we were only able to obtain rates from 13.8 to 38.2 °C (a range of 25.1 °C) in this solvent. To obtain reliable values for $\Delta S^{\ddagger}$, a range of at least 40 °C is recommended. The activation parameters were thus measured in benzene from rates obtained over a wider temperature range of 37.2 °C (7.0 to 44.2 °C), and similar values for the activation parameters were obtained ($\Delta H^{\ddagger}$ = 15.5(3) kcal mol^{-1} and $\Delta S^{\ddagger}$ = −3.3(11) eu; see the Supporting Information).

(13) Errors in the activation parameters were calculated using previously derived equations: Morse, P. M.; Spencer, M. D.; Wilson, S. R.; Girolami, G. S. *Organometallics* **1994**, *13*, 1646−1655.

(14) (a) Eaton, D. R.; Phillips, W. D.; Caldwell, D. J. *J. Am. Chem. Soc.* **1963**, *85*, 397−406. (b) Sacconi, L.; Paoletti, P.; Ciampolini, M. *J. Am. Chem. Soc.* **1963**, *85*, 411−416. (c) Holm, R. H.; Chakravorty, A.; Dudek, G. O. *J. Am. Chem. Soc.* **1964**, *86*, 379−387. (d) Chakravorty, A.; Holm, R. H. *J. Am. Chem. Soc.* **1964**, *86*, 3999−4004. (e) Everett, G. W., Jr.; Holm, R. H. *J. Am. Chem. Soc.* **1965**, *87*, 2117−2128. (f) Shupack, S. I. *J. Inorg. Nucl. Chem.* **1966**, *28*, 2418−2419. (g) Ernst, R. E.; O'Connor, M. J.; Holm, R. H. *J. Am. Chem. Soc.* **1967**, *89*, 6104−6113. (h) Everett, G. W.; Holm, R. H. *Inorg. Chem.* **1968**, *7*, 776−785. (i) Pignolet, L. H.; Horrocks, W. E., Jr. *J. Am. Chem. Soc.* **1968**, *90*, 922−926. (j) Gerlach, D. H.; Holm, R. H. *J. Am. Chem. Soc.* **1969**, *91*, 3457−3467. (k) La Mar, G. N.; Sherman, E. O. *J. Am. Chem. Soc.* **1970**, *92*, 2691−2699. (l) Que, L., Jr.; Pignolet, L. H. *Inorg. Chem.* **1973**, *12*, 156−163. (m) Knoch, R.; Elias, H.; Paulus, H. *Inorg. Chem.* **1995**, *34*, 4032−4040. (n) Simon-Manso, E.; Valderrama, M.; Boys, D. *Inorg. Chem.* **2001**, *40*, 3647−3649. (o) Brusko, V. V.; Rakhmatullin, A. I.; Shtyrlin, V. G.; Krivolapov, D. B.; Litvinov, I. A.; Zabirov, N. G. *Polyhedron* **2006**, *25*, 1433−1440. (p) Mori, Y.; Shirase, H.; Fukuda, Y. *Bull. Chem. Soc. Jpn.* **2008**, *81*, 1108−1115. (q) Starikov, A. G.; Minyaev, R. M.; Minkin, V. I. *Chem. Phys. Lett.* **2008**, *459*, 27−32.

(15) Eaton, D. R. *J. Am. Chem. Soc.* **1968**, *90*, 4272−4275.

(16) Halevi, E. A.; Knorr, R. *Angew. Chem., Int. Ed.* **1982**, *21*, 288−289.

(17) For a few examples, see: (a) Albright, T. A.; Hoffmann, R.; Thibeault, J. C.; Thorn, D. L. *J. Am. Chem. Soc.* **1979**, *101*, 3801−3812. (b) Redfield, D. A.; Nelson, J. H. *Inorg. Chem.* **1973**, *12*, 15−19. (c) Romeo, R.; Plutino, M. R.; Elding, L. I. *Inorg. Chem.* **1997**, *36*, 5909−5916. (d) Bartolome, C.; Espinet, P.; Martin-Alvarez, J. M.; Villafane, F. *Eur. J. Inorg. Chem.* **2004**, 2326−2337. (e) Yang, F.-Z.; Wang, Y.-H.; Chang, M.-C.; Yu, K.-H.; Huang, S.-L.; Liu, Y.-H.; Wang, Y.; Liu, S.-T.; Chen, J.-T. *Inorg. Chem.* **2009**, *48*, 7639−7644.

(18) Redfield, D. A.; Nelson, J. H. *J. Am. Chem. Soc.* **1974**, *96*, 6219−6220.

(19) Crabtree, R. H. *The Organometallic Chemistry of the Transition Metals*, 4th ed.; Wiley-Interscience: Hoboken, NJ, 2005; pp 104−112.

(20) Collman, J. P.; Hegedus, L. S.; Norton, J. R.; Finke, R. G. *Principles and Applications of Organotransition Metal Chemistry*; University Science Books: Mill Valley, CA, 1987; p 247.

(21) (a) Kappes, M. M.; Staley, R. H. *J. Am. Chem. Soc.* **1982**, *104*, 1813−1819. (b) Hettich, R. L.; Jackson, T. C.; Stanko, E. M.; Freiser, B. S. *J. Am. Chem. Soc.* **1986**, *108*, 5086−5093. (c) Jacobson, D. B.; Freiser, B. S. *J. Am. Chem. Soc.* **1983**, *105*, 7492−7500.

(22) Brookhart, M; Green, M. L. H.; Parkin, G. *Proc. Natl. Acad. Sci. U.S.A.* **2007**, *104*, 6908−6914.

(23) Kogut, E.; Zeller, A.; Warren, T. H.; Strassner, T. *J. Am. Chem. Soc.* **2004**, *126*, 11984−11994.

(24) This does not necessarily discount the presence of paramagnetic nickel(II), because standard EPR spectroscopy at conventional microwave frequencies can be ineffective for detecting transition metals with integer spin ground states: Krzystek, J.; Park, J.-H.; Meisel, M. W.; Hitchman, M. A.; Stratemeier, H.; Brunel, L.-C.; Telser, J. *Inorg. Chem.* **2002**, *41*, 4478−4487.

(25) (a) Schubert, E. M. *J. Chem. Educ.* **1992**, *69*, 62. (b) Evans, D. F. *J. Chem. Soc.* **1959**, 2003−2005.

(26) Frisch, M. J. , et al. *Gaussian 09, Revision A.02*; Gaussian, Inc., Wallingford, CT, 2009.

(27) JIMP2, version 0.091, a free program for the visualization and manipulation of molecules: (a) Hall, M. B.; Fenske, R. F. *Inorg. Chem.* **1972**, *11*, 768. (b) Manson, J.; Webster, C. E.; Hall, M. B. Texas A&M University, College Station, TX, 2006; http://www.chem.tamu.edu/jimp2/index.html.